Surface organization and nanopatterning of collagen by dip-pen nanolithography

Donna L. Wilson*, Raquel Martin*, Seunghun Hong†, Mark Cronin-Golomb‡, Chad A. Mirkin†, and David L. Kaplan*§

Departments of *Chemical and Biological Engineering and Bioengineering Center, and ‡Electrical Engineering and Computer Science and Bioengineering Center, Tufts University, Medford, MA 02155; and †Northwestern University, Department of Chemistry, Evanston, IL 60208-3113

Edited by S. Walter Englander, University of Pennsylvania School of Medicine, Swarthmore, PA, and approved September 27, 2001 (received for review June 26, 2001)

Collagen is a key fibrous protein in biological systems, characterized by a complex structural hierarchy as well as the ability to self-assemble into liquid crystalline mesophases. The structural features of collagen influence cellular responses and material properties, with importance for a wide range of biomaterials and tissue architectures. The mechanism by which fibrillar collagen structures form from liquid crystalline mesophases is not well characterized. We report positive printing of collagen and a collagen-like peptide down to 30–50-nm line widths, using the atomic force microscopy technique of dip-pen nanolithography. The method preserved the triple-helical structure and biological activity of collagen and even fostered the formation of characteristic higher levels of structural organization. The ''direct-write'' capability of biologically relevant molecules, while preserving their structure and functionality, provides tremendous flexibility in future biological device applications and in proteomics arrays, as well as a new strategy to study the important hierarchical assembly processes of biological systems.

The controlled construction of supramolecular inorganic, organic, and biological materials is an area of intense research. Nature accomplishes the construction of well organized materials through the process of self-assembly, relying on noncovalent and covalent interactions between relatively small precursor molecules (1). This ''bottom-up'' approach to supramolecular organization, driven by self-assembly, leads to unusual and important properties in biologically derived materials. Although these processes are not well understood, they seem to be critical in the biological assembly of complex material systems such as tough mineralized matrices (organic-inorganic) in shells and bone to complex architectures in extracellular matrices (organic-organic).

One approach that can be taken to gain additional insight into these processes is to simplify complex three-dimensional assemblies into two-dimensional (2D) patterns. Patterning a monolayer of precursor ''director'' molecules on length scales ranging from nanometer to micrometer should simplify the interpretation of supramolecular assembly formation and organization (2, 3). As an example of 2D assembly, the influence of self-assembled monolayers on cell attachment and spreading is of fundamental and applied importance (4). These processes are mediated by proteins in the extracellular matrix (ECM), such as fibronectin, laminin, and collagen. Command over attachment of cells to a surface relies on orientational control of ECM protein surface adsorption and molecule conformation (5–7). This relationship between surface features and cells directly influences cell metabolism, communicated from membrane (integrin) receptors via cytoskeletal and biochemical networks to influence cell growth and extracellular matrix formation. This control has important implications in areas such as single cell manipulation, toxicology, and drug screening, as well as biomaterial structures and function (8).

Collagen is a useful molecule to pattern because of its fibrillar assembly and organization *in vivo* and *in vitro*, an ability to form liquid crystalline mesophases, and its architectural influence on a wide range of biomaterials and tissue architectures ranging from fibrous connective tissues and bone to mesh-like basement membranes (9). The basic helical repeat (glycine-proline-hydroxyproline and variants on this repeat) drives hierarchical assembly programmed at the level of primary sequence leading to complex structural arrays. Additionally, collagen-like model peptides, in lieu of the larger native proteins, have the advantage of being ''sequence-specific'' while at the same time mimicking the triple-helical nature of the collagen molecule, often stimulating the same cell behavior as the native and longer counterparts (10–12). Thus, valuable insights into collagen patterning behavior can be examined by constructing various collagen-like model peptides whose repetitive sequence is altered in a systematic pattern (13).

A variety of surface-patterning molecular lithographic techniques has been explored to achieve two-dimensional organization of molecules (14). Microcontact printing (μCP; refs. 15–17), atomic force microscopy (AFM)-based techniques of dip-pen nanolithography (DPN; refs. 18–20), and scanning probe lithography (21, 22) have been used successfully in the preparation of structures on the nanometer- to micrometer-length scales. We report positive printing at the nanometer scale of large free-standing collagen and collagen-like peptide molecules by means of DPN. These molecules have been patterned with line widths as small as 30–50 nm, the largest molecules thus far positively printed on a surface at such small-length scales. Additionally, hierarchical self-assembly may be induced by means of the DPN method as a result of the combination of AFM tip contact and surface frictional forces. It is hypothesized that a localized concentration of solution occurs as the tip translates the surface. The thin needle-like shape of the tip is able to induce a confined liquid crystalline-like organization in a process similar to fiber drawing. Writing with large polymers, such as collagens and collagen-like peptides, provides new options in materials patterning and function, as well as insight into molecular self-assembly.

Materials and Methods

Preparation of Au (111) Substrates. Substrates were prepared by using muscovite green mica wafers (Ted Pella, Redding, CA). The mica was coated with ≈300 nm of 99.99% Au (Electron Microscopy Sciences, Fort Washington, PA) by means of evaporation with a thermal evaporator. The Au substrates were either used immediately or stored under dry sterile conditions for no longer than 10 days.

This paper was submitted directly (Track II) to the PNAS office.

Abbreviations: DPN, dip-pen nanolithography; CD, circular dichroism; NSOM, near-field optical microscopy/microscope; AFM, atomic force microscopy; TESP, TappingMode etched silicon probe.

§To whom reprint requests should be addressed at: Department of Chemical and Biological Engineering and Bioengineering Center, Tufts University, 4 Colby Street, Room 125, Medford, MA 02155. E-mail: david.kaplan@tufts.edu.

The publication costs of this article were defrayed in part by page charge payment. This article must therefore be hereby marked "*advertisement*" in accordance with 18 U.S.C. §1734 solely to indicate this fact.

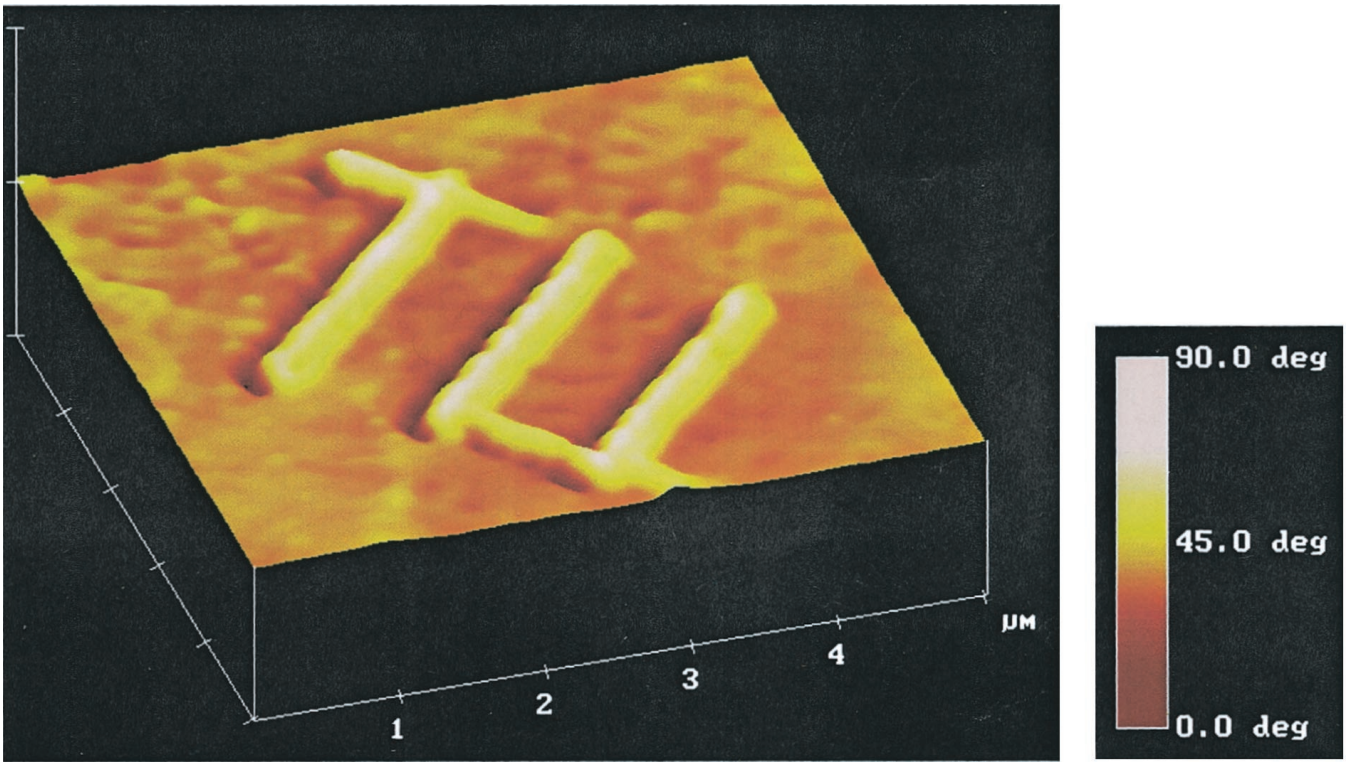

Fig. 1. Phase image of thiolated collagen on Au substrate. The uniform deposition and 120 ± 1.6 nm line widths can be easily visualized. The AFM tip was immersed in ≈1 mg/ml of 1 mM HCl aqueous solution of the thiolated native collagen (pH 3.0). DPN was performed at a force 0.1 nN with a scan rate of 0.002 Hz. Imaging was achieved in a 6-μm scan width at a rate of 2.0 Hz on Au-evaporated surfaces. Repeated scanning in tapping mode did not disturb the patterned images.

Preparation of Thiolated Collagen. Thiolation of the collagen was achieved by using lyophilized rat tail tendon collagen (Roche Molecular Biochemicals) at a concentration of 2 mg/ml reconstituted in 1.0 mM HCl, pH 3.0 (23, 24). The pH was maintained throughout the experiment to sustain collagen solubility. Cystamine (Sigma) was added to a concentration of 1.0 M, and initiation of the reaction was through the addition of 1-ethyl-3-(3-dimethylaminopropyl)carbodiimide (ECD) (Sigma) to a concentration of 2.0 M. The reaction ran for 3 h at 4°C with stirring and then was dialyzed extensively against 4 liters of 1.0 mM HCl also at 4°C. The collagen was then reduced by addition of DTT (Sigma) to a final concentration of 6.0 mM for 20–30 min at 4°C. Again, extensive dialysis against 4 liters of 1.0 mM HCl (pH 3.0) was performed. Collagen concentrations of ≈1.0 mg/ml were used for DPN experiments.

Solid Phase Ab Binding. Collagen-patterned substrates were washed with 3% BSA in PBS, pH 7.4, containing 0.02% sodium azide as blocking buffer. Substrates were then soaked in the blocking solution for 20 min at room temperature. Rabbit anti-mouse collagen primary Ab (Research Diagnostics, Flanders, NJ) solution at a 1:50 dilution in blocking buffer was incubated with the substrates in a humidified atmosphere for 2 h. The substrates were again washed with blocking buffer solution as before. Alexa Fluor 488 goat anti-rabbit IgG (H + L) conjugate (Molecular Probes) secondary Ab solution at 5 μg/ml in blocking buffer was incubated with the substrates as with the primary Ab for 20 min. The substrates were washed extensively after incubation with the blocking buffer to remove any unbound Ab.

Circular Dichroism (CD) Spectroscopy of Collagen and Collagen-Like Peptides. The triple-helical structure of collagen and collagen-like peptides was monitored by means of CD studies. Solution-state CD studies were performed on a Jasco (Easton, MD) J-710 Spectropolarimeter. Solution concentrations were 1 mg/ml of protein in water, with a path length of 0.1 cm at 25°C. For the collagen, spectra were taken before and after thiolation to detect structural changes. CD spectra were analyzed by using a neural network-based deconvolution program, CDNN (25), and compared with literature values.

Preparation of Collagen Peptide. A collagen-like peptide [Cys(Glu)$_5$(GlyAlaHypGlyProHyp)$_6$(Glu)$_5$, where Hyp is hydroxyproline] was synthesized via f-moc chemistry (Tufts Univ. School of Medicine Core Protein Chemistry Facility) and dissolved in ≈40 mg/ml of aqueous solutions. The triple-helical content of the peptide was determined by CD as described earlier.

AFM Tip Preparation. The AFM tips were "inked" by dipping into aqueous solutions of the modified protein or the peptide. The AFM tip was immersed in a ≈40-mg/ml aqueous solution of peptide or ≈1 mg/ml of 1 mM HCl aqueous solution of the thiolated native collagen (pH 3.0). For most experiments, coating the Si tip was unnecessary, and the tip was immersed in the solution for ≈2 min (26).

Atomic Force Microscope Imaging and Manipulation. All imaging and lithography were performed in TappingMode on a Dimension 3100 Nanoscope III with TappingMode etched silicon probes (TESP), rotated TESP, or IBM Super cone probes (ISCP) (Digital Instruments, Santa Barbara, CA). TESP probes have a cantilever length of 225 μm and a spring constant of 1–5 N/m. Rotated TESP AFM tips have the same spring constants and cantilever lengths as the TESP probes except that the tips rotated at a 15° angle so that high-aspect ratio features can be more easily

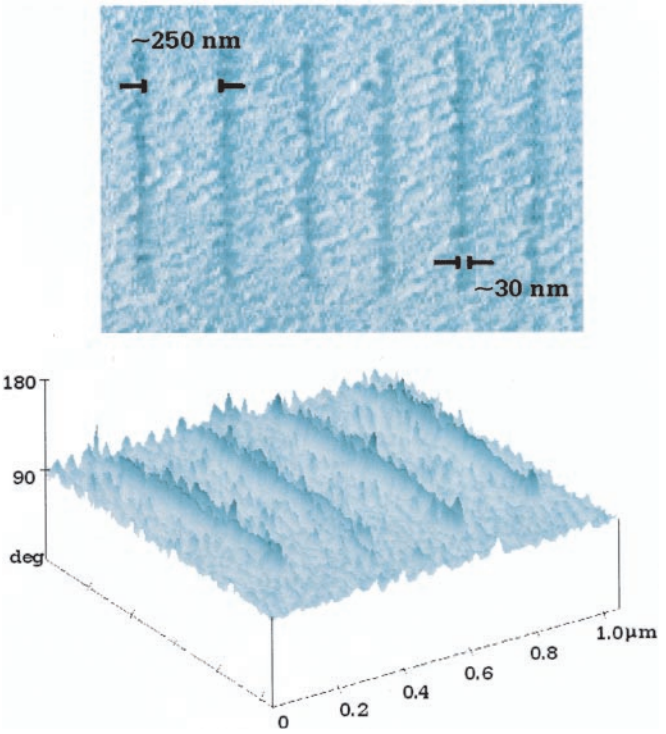

Fig. 2. Phase image of patterned collagen at 30 ± 4.6-nm line widths. Lines were achieved by using probes with a cantilever length of 125 μm with a spring constant of 50–200 N/m developed specifically to measure high-aspect ratio features. Phase images are obtained by mapping the phase of the cantilever oscillation during the tapping-mode scan. Therefore, phase imaging detects variations in composition, adhesion, friction, and viscoelasticity. Imaging was achieved in a 3-μm scan width at a rate of 2.0 Hz.

visualized. ISCP probes cantilever length is 125 μm with a spring constant of 50–200 N/m developed specifically to measure high-aspect ratio features. Parallel lines were made at forces varying from 0.50 nN and a step of 0.05 nN with a scan rate of 0.002 Hz. Imaging was achieved in a 3-μm scan width at a rate of 2.0 Hz.

Near-Field Scanning Optical Microscopy (NSOM). NSOM reflective mode images of the collagen patterns were obtained with an NSOM operating under ambient temperatures and pressures by using an NSOM-100 Digital Instruments Interface Module and Integrator (Nanonics, Phoenix) coupled with a Nikon optical microscope under electronic control of a Nanoscope IIIa Scanning Probe Microscope Controller (Digital Instruments). Scanning probe cantilevered near-field optical tips (Nanonics) at an average resonant frequency of 139 kHz were used. The fluorescence was excited through the NSOM tip with the 488-nm line of a Coherent Innova Enterprise II argon ion laser (Coherent Radiation, Palo Alto, CA). Imaging of molecule patterns was obtained in tapping mode at an approximate rate of 1.0 Hz.

Results

Nanolithography of Collagen. The spatially controlled patterning of thiolated collagen molecules is evident in Fig. 1. Lithography of the collagen molecule on a variety of length scales was accomplished indicating that large-molecule patterning can cover a range up to ≈100 μm in length and ≈800 nm in width per line. Small-dimension lines of 30–40 nm in width and 100 nm in length were written on the gold substrates at a spacing of 250 nm by using DPN techniques in Fig. 2; however, higher levels of

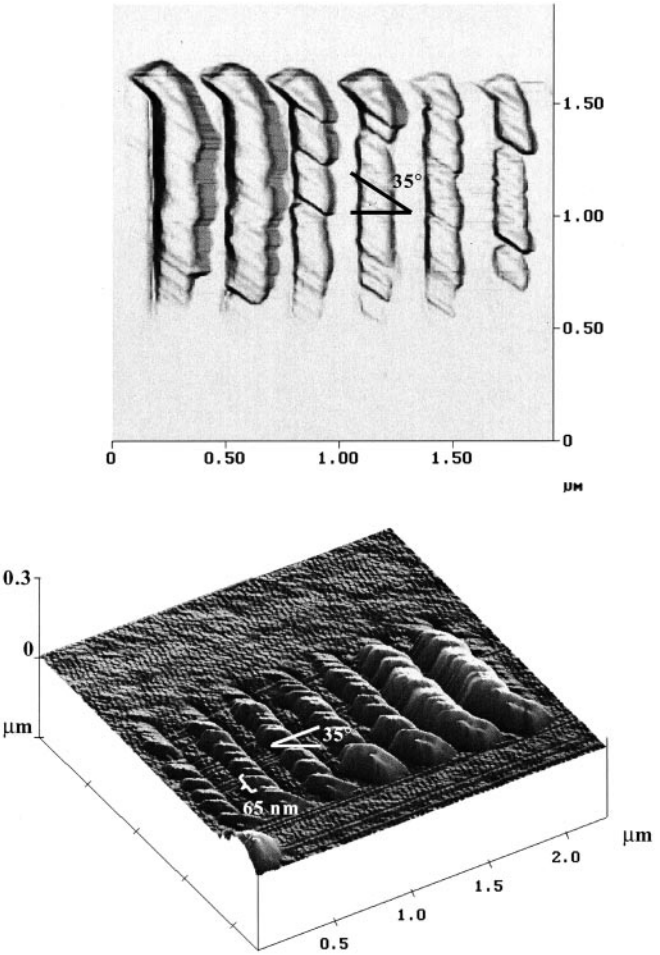

Fig. 3. Top and surface plot views of a topography image of modified collagen molecules deposited on Au substrates at varying forces by using the same tip inked once in collagen solution. Note the 35°, 65-nm periodicity observed along the long axis of the lines, as well as the 300-nm height of the molecules. Rotated TESP AFM tips have a cantilever length of 225 μm and a spring constant of 1–5 N/m rotated at a 15° angle so that high-aspect ratio features can be easily visualized. Parallel lines were made at forces varying from 0.50 nN and a step of 0.05 nN with a scan rate of 0.002 Hz. Imaging was achieved in a 3-μm scan width at a rate of 2.0 Hz. Scan angle did not change the directional orientation of the patterns.

organization at these line widths were not observed. The thiolation modification of collagen was necessary to ensure coupling to the gold surface. The sulfhydryl addition results in firm attachment of the collagen to the gold substrate as verified by repeated washing of the surface, creating a stable surface pattern. No persistent patterning was observed in the absence of the thiolation.

The use of tapping-mode AFM for the imaging and lithography was essential as a result of the sensitivity of proteins to the shear and frictional forces required to interrogate the surface in contact mode. The results demonstrate that tapping mode can be successfully used with DPN to fabricate large biological molecules on surfaces. Complementary in sensitivity to the friction image obtained with the AFM operating in lateral force mode or contact mode (27) is the phase image obtained in tapping mode. Because both phase and friction images are highly sensitive (28), it is important to verify that the desired molecules are deposited and that the image is not a result of solvent deposition during the lithography process (27).

The collagen type I triple helix is ≈3000 Å long and ≈14 Å

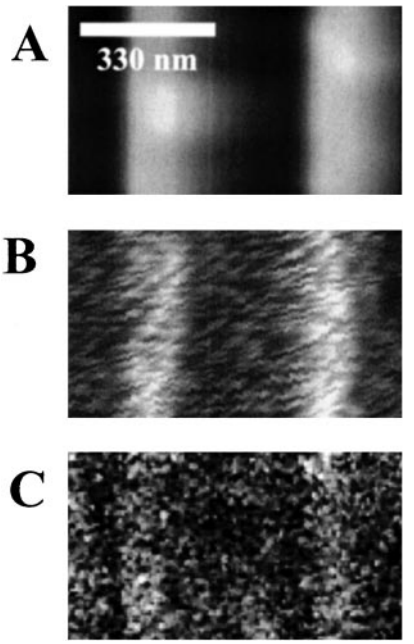

Fig. 4. AFM topography image of collagen patterns without Ab binding (*A*); an NSOM topography image of same collagen pattern with Ab binding (*B*); and an NSOM image of same collagen pattern with Ab binding (*C*). NSOM fluorescence image was obtained at an excitation wavelength of 488 nm, and lines observed in *C* correspond to Ab fluorescence.

wide. Topography image data revealed heights up to ≈300 nm (Fig. 2). Because the triple helix of the collagen molecule can be modeled as a rigid rod, the length of the molecule energetically favors orientation along the long axis of the AFM tip. Although the higher height values observed correspond to the collagen height recognized for the length that can be maintained as rigid rods (50–200 nm) (9), it is possible for the molecules to sample a variety of orientations relative to the surface as a result of the multiple thiol groups decorating the chains. This conclusion is supported by the helical repeat observed in Fig. 3.

The helical architecture of the patterned two-dimensional assembled proteins is particularly striking (Fig. 3). A periodicity of 65 ± 3.4 nm at a 35 ± 0.7° angle is evident along the long axis of the patterned lines, suggesting that the patterning process drives the regular helical structural organization of the molecules (29). One explanation for this observation is that as a first molecule comes into contact with the gold substrate through a diffusive process, a large portion of the molecule is still interacting with tip-associated molecules. As the tip translates across the surface, the next molecule is pulled into alignment with the previous molecule already on the surface based on natural self-assembly mechanisms involved during the hierarchical assembly of collagen *in vivo*. Furthermore, the similarity of this observed higher-order helical pattern, with the characteristic 64-nm repeats observed for native collagen assemblies by electron microscopy, suggests that native-like hierarchical assembly of the collagen is preserved and perhaps even facilitated during the nanopatterning process. When compared with AFM images of the same collagen solution dropped from bulk solution onto the Au surface, no regular patterns or periodicities were observed (data not shown). The additional fact that the helical periodicity of the lines does not change with alterations in tip force further suggests a native assembly process arising from the lithographic technique.

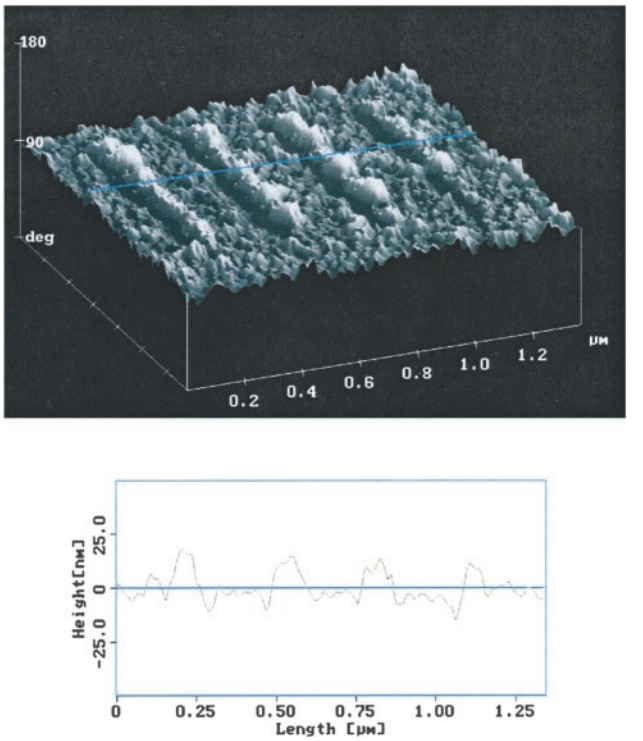

Fig. 5. Topography image of a collagen-like peptide for lines 1 μm in length and 30-nm in width. The collagen-like peptide [Cys(Glu)$_5$(Gly-AlaHypGlyProHyp)$_6$(Glu)$_5$, where Hyp is hydroxyproline] was dissolved in ≈40 mg/ml of aqueous solution. The triple-helical content of the peptide was determined by CD before patterning. The uniform height observed in the topography images corresponds to the ≈15-nm height of the peptide triple helix. DPN was performed in the same manner as described for the collagen molecule.

Verification of Active Collagen Conformation via NSOM. To determine whether the patterned proteins retained native collagen-like structure, and thus biological activity, reactions with a collagen-specific primary Ab and a secondary fluorescent Ab specific for the primary were used to probe the nanopatterns. Preliminary fluorescence studies demonstrated that the modified collagen was specifically labeled (data not shown), verifying that the protein retained specificity and epitope display after thiolation. Patterned images taken after Ab labeling via NSOM revealed fluorescence image spacing matching the line spacing obtained in the original topography image of the pattern before Ab binding (Fig. 4), confirming retention of Ab reactivity after lithographic patterning as well. This specificity in recognition by a collagen-specific Ab after thiolation and nanopatterning is critical as a segue into advanced materials patterning with biological relevance. These data also suggest a means for "trapping" or "docking" molecules that otherwise might present difficulties in patterning directly, but in which organized arrays are desirable. In other words, nanopatterns could be used to guide the deposition and assembly of additional assemblies into three dimensions.

Nanolithography of Collagen Model Peptides. Nanolithography of a collagen-like peptide was also accomplished at line widths of ≈30–40 nm and lengths of 100 nm with a 250-nm spacing, as well as for larger surface areas (Fig. 5). The central region of the peptide, similar to the primary amino acid sequence found in native collagen, corresponds to the triple-helical domain and contains a glycine at every third position and a high proportion of proline and hydroxyproline in the second and

third positions. An N-terminal cysteine was incorporated for chemisorption to the Au substrate. Attachment was established by means of washing and reimaging experiments of the patterned regions, resulting in both reproducible topography and phase images.

The collagen-like peptides spontaneously assembled into homotrimeric triple helices in aqueous solution as confirmed by CD. These peptides may, therefore, be modeled as rigid rods and are expected to behave in much the same manner as the collagen molecule with respect to orientation along the long axis of the AFM tip. A simple calculation of rise per residue, as compared with that of the native collagen triple-helical domain, results in an estimated height of ≈15 nm for the polypeptides. This height corresponds to the 12–17-nm heights observed in topography images of the collagen-like peptide-patterned Au substrates, indicating the presence of these molecules in the nanoarrays and the terminal end contact of the molecules with the surface.

Discussion

The suggestion that the DPN lithographic process might facilitate native self-assembly processes could lend further insight to how such processes occur and offer options for extending this capability to other self-assembling molecules. The nature of the molecular organization in the patterns should be influenced by humidity, temperature, and concentration, and future work should explore these variables in a systematic manner.

Additionally, nanopatterning of collagen molecules has significant implications in extending DPN technology to molecules of biological importance as well as polymers in general. The sensitivity of these types of biological molecules to thermally induced structural changes (e.g., denaturation) makes the DPN lithographic method ideal in comparison to harsher techniques such as ion-beam-based lithography. Specific nanopatterned arrays of collagen might be used to induce an assembly network of collagen scaffoldings to mediate cell attachment processes, organized as optical gratings because of their ability to form liquid crystalline phases, and as guest-host systems for other biological or nonbiological components. For example, recent success with high-density spatial arrays of proteins at ≈0.2 mm resolution (30) to study protein function would benefit from the orders of magnitude-improved resolution described in the present study for higher density arrays achieved by "writing." The findings that DPN can be used to pattern collagen and collagen-like peptides at the nanoscale offers new options for this technique in a variety of fundamental and applied areas of materials science and biology.

We thank the National Aeronautics and Space Administration and the Air Force Multidisciplinary University Research Initiative program for support of this effort. We also thank Peggy Cebe of Tufts University for help with preparation of the gold substrates.

1. McGrath, K. & Kaplan, D. (1997) in *Protein-Based Materials*, ed. Kaplan, D. (Birkhauser, Basel).
2. Mirkin, C. A. (2000) *Inorg. Chem.* **39,** 2258–2272.
3. Lowe, C. R. (2000) *Curr. Opin. Struct. Biol.* **10,** 428–434.
4. Guetens, G., van Cauwenberghe, K., De Boeck, G., Maes, R., Tjaden, U. R., van der Greef, J., Highly, M., van Oosterom, A. T. & de Bruijn, E. A. (2000) *J. Chromatogr. B* **739,** 139–150.
5. Burmeister, J. S., Vrany, J. D., Reichert, W. M. & Truskey, G. A. (1996) *J. Biomed. Mater. Res.* **30,** 13–22.
6. Iuliano, D. J., Saavedra, S. S. & Truskey, G. A. (1993) *J. Biomed. Mater. Res.* **27,** 1103–1113.
7. Ito, Y. (1999) *Biomaterials* **20,** 2333–2342.
8. Mrksich, M. & Whitesides, G. M. (1996) *Annu. Rev. Biophys. Biomol. Struct.* **25,** 55–78.
9. Kuhn, K., Glanville, R., Wilfried, B., Qian, R.-Q., Dieringer, H., Voss, T., Siebold, B., Oberbaumer, I., Schwarz, U. & Yamada, Y. (1985) in *Biology, Chemistry, and Pathology of Collagen*, eds. Fleischmajer, R., Olsen, B. R. & Kuhn, K. (N.Y. Acad. Sci., New York), Vol. 460, pp. 14–24.
10. Anthony-Cahill, S. J., Benfield, P. A., Fairman, R., Wasserman, Z. R., Brenner, S. L., Stafford, W. F., Altenbach, C., Hubbell, W. L. & DeGrado, W. F. (1992) *Science* **255,** 979–983.
11. Betz, S., Fairman, R., O'Neil, K., Lear, J. & Degrado, W. (1995) *Philos. Trans. R. Soc. London B* **348,** 81–88.
12. Bryson, J. W., Desjarlais, J. R., Handel, T. M. & DeGrado, W. F. (1998) *Protein Sci.* **7,** 1404–1414.
13. Degrado, W. F. (1988) *Adv. Protein Chem.* **39,** 51–124.
14. Berggren, K. K., Bard, A., Wilbur, J. L., Gillaspy, J. D., Helg, A. G., McClelland, J. J., Rolston, S. L., Phillips, W. D., Prentiss, M. & Whitesides, G. M. (2000) *Science* **260,** 1255–1257.
15. Jackman, R. J., Wilbur, J. L. & Whitesides, G. M. (1995) *Science* **269,** 664–666.
16. Yan, L., Zhao, X.-M. & Whitesides, G. M. (1998) *J. Am. Chem. Soc.* **120,** 6179–6180.
17. Kane, R. S., Takayama, S., Ostuni, E., Ingber, D. E. & Whitesides, G. M. (1999) *Biomaterials* **20,** 2363–2376.
18. Hong, S., Zhu, J. & Mirkin, C. A. (1999) *Science* **286,** 523–525.
19. Hong, S. & Mirkin, C. A. (2000) *Science* **288,** 1808–1811.
20. Piner, R. D., Zhu, J., Xu, F., Hong, S. & Mirkin, C. A. (1999) *Science* **283,** 661–663.
21. Liu, G.-Y., Song, X. & Qian, Y. (2000) *Acc. Chem. Res.* **33,** 457–466.
22. Amro, N. A., Song, X. & Liu, G.-Y. (2000) *Langmuir* **16,** 3006–3009.
23. Lin, C., Miahl, K. A. & Krueger, R. J. (1990) *Biochim. Biophys. Acta* **1038,** 382–385.
24. Fattom, A. V., Vann, W. F., Szu, S. C., Sutton, A., Li, X., Bryla, D., Schiffman, G., Robbins, J. B. & Schneerson, R. (1988) *Infect. Immun.* **56,** 2292–2298.
25. Böhm, G. (1997) CDNN, CD Spectra Deconvolution (Univ. of Halle-Wittenberg, Halle, Germany), Version 2.1.
26. Piner, R. D., Hong, S. & Mirkin, C. A. (1999) *Langmuir* **15,** 5457–5460.
27. Colton, R. (1998) *Procedures in Scanning Probe Microscopies* (Wiley, West Sussex, England).
28. Piner, R. D., Hong, S. & Mirkin, C. A. (1997) *Langmuir* **13,** 6864–6868.
29. Kadler, K. E., Holmes, D. F., Trotter, J. A. & Chapman, J. A. (1996) *Biochem. J.* **316,** 1–11.
30. MacBeath, G. S. & Stuart, L. (2000) *Science* **289,** 1760–1763.